Eur. J. Mineral.
2002, **14**, 513-524

Geochronological constraints on the timing of migmatization in the Dabie Shan, East-central China

JIANG-HAI WANG[1]*, MIN SUN[2] and SHANG-XIAN DENG[1]

[1]Guangzhou Institute of Geochemistry, Chinese Academy of Sciences, P.O. Box 1131, Guangzhou 510640, P.R. China
[2]Department of Earth Sciences, The University of Hong Kong, Pokfulam Road, Hong Kong, P.R. China

Abstract: Combined isotopic dating techniques reveal a complicated tectonothermal history for the migmatites at Fenghuangguan and Zongluzui in the Northern Dabie Unit (NDU). The zircon U-Pb data indicate that the rocks were migmatized about 131.7 ± 1.1 Ma ago. Two whole-rocks (leucosome and melanosome) and three mineral separates yield an internal Rb-Sr isochron age of 115 ± 2 Ma. The $^{40}Ar/^{39}Ar$ step-heating analyses for four leucosomes give isochron ages of 114 ± 1 Ma and 111 ± 1 Ma for hornblende, 107 ± 0.5 Ma for biotite and 95 ± 2 Ma for K-feldspar. These data indicate that the NDU was uplifted after the migmatization at a cooling rate of 10-12°C/Ma. Biotite $^{40}Ar/^{39}Ar$ step-heating analyses for a felsic granulite at Huangtuling give an isochron age of 194 ± 2 Ma and a plateau age of 195 ± 2 Ma, suggesting that the granulite facies metamorphism predated the regional migmatization. Decoupling between the Rb-Sr age for biotite and $^{40}Ar/^{39}Ar$ ages for hornblende is interpreted as recrystallization induced by a fluid action. The migmatization is considered as one result of the extensive thermal event in east China, also resulting in the Yanshanian magmatic activities. The previously published isotopic ages of about 130 Ma for the orthogneisses in the NDU may simply record this thermal event. The Nd and Sr isotopic data indicate the existence of pre-Cretaceous, or even Precambrian rocks in the NDU.

Key-words: geochronology, migmatization, Dabie Shan.

1. Introduction

The Dabie Shan metamorphic complex in east-central China contains ultrahigh pressure rocks that resulted from continental collision between the Sino-Korean Craton in the north and the Yangtze Craton in the south (Fig. 1). This complex can be divided into three fault-bounded tectonic units: the Southern Dabie Unit (SDU), the Central Dabie Unit (CDU) and the Northern Dabie Unit (NDU) (Fig. 2). The SDU is composed of lower amphibolite-facies and blueschist-facies metamorphic rocks, which underwent high-pressure (HP) metamorphism (*e.g.*, Suo *et al.*, 1993). Diamond- and coesite-bearing rocks were identified in the CDU, demonstrating up to 4.0 GPa ultrahigh-pressure (UHP) metamorphism for this unit (Okay *et al.*, 1989; Wang *et al.*, 1989; Xu *et al.*, 1992; Maruyama *et al.*, 1994; Liou *et al.*, 1996). In contrast, the NDU consists dominantly of high-temperature (HT) metamorphic rocks of upper amphibolite to granulite facies (Fig. 2). High-quality geochronological data are critical for understanding the formation and tectonic history of these metamorphic rocks. Previous geochronological studies were mostly focused on the HP-UHP rocks (*e.g.*, Li *et al.*, 1989, 1993; Chen *et al.*, 1992; Eide *et al.*, 1994; Ames *et al.*, 1996; Chavagnac & Jahn, 1996; Rowley *et al.*, 1997) and a general consensus has recently been reached that the HP-UHP metamorphism took place between about 210 and 230 Ma (*e.g.,* Liou *et al.*, 1996). Some geochronological studies have also been conducted on granulites (*e.g.*, Li *et al.*, 1993; Jian *et al.*, 1997), deformed orthogneisses, undeformed granitic plutons (*e.g.*, Chen *et al.*, 1991; Li & Wang, 1991; Chen *et al.*, 1995; Rowley *et al.*, 1997; Xue *et al.*, 1997; Hacker *et al.*, 1998; Chen *et al.*, 2000; Zheng *et al.*, 2000) and Cretaceous post-collisional mafic-ultramafic plutonic rocks such as gabbro and pyroxenite (*e.g.*, Hacker *et al.*, 1998; Ge *et al.*, 1999; Jahn *et al.*, 1999; Li *et al.*, 1999; Chen *et al.*, 2000). However, the important thermal event recorded by the migmatites in the NDU has not been constrained. Consequently, several key problems such as the temporal relationship between the HT and HP-UHP metamorphism and the spatial relationship between NDU and the CDU/SDU remain mysterious. This paper provides new zircon U-Pb, Sm-Nd, Rb-Sr and $^{40}Ar/^{39}Ar$ isotopic data, constrains the timing of migmatization, discusses the HT metamorphism in the NDU, and highlights the tectonic relationship of the NDU with the CDU/SDU.

* Corresponding author: e-mail: wangjh@gig.ac.cn

0935-1221/02/0014-0513 $ 5.40
DOI: 10.1127/0935-1221/2002/0014-0513

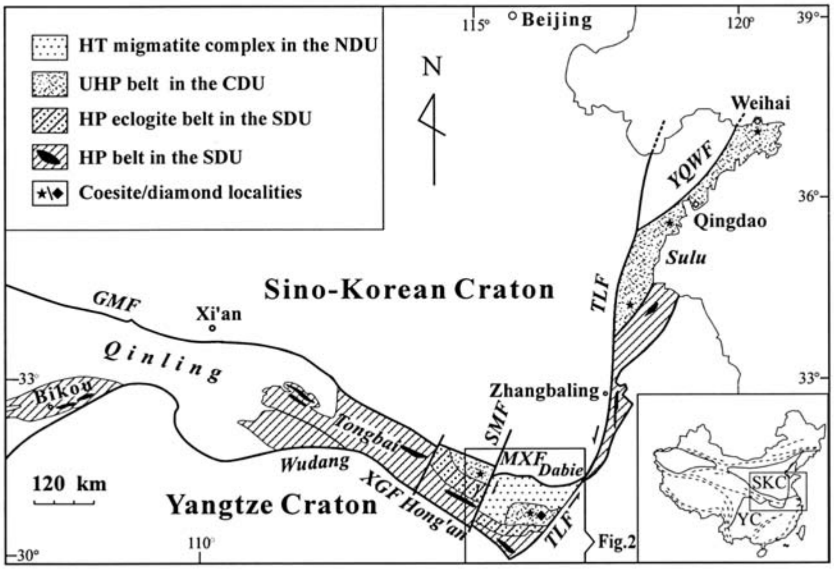

Fig. 1. Regional tectonic map of the Qinling-Dabie collisional zone between the Sino-Korean Craton (SKC) and Yangtze Craton (YC) in east-central China. Note the segmentation and displacement of the tectonic units by the Tan-Lu fault (TLF) and other faults into several blocks, including the Sulu, Dabie, Hong'an, Wudang, Tongbai and Bikou Blocks. The UHP belt is north of the HP belt. Blueschists are discontinously exposed in the HP belt for more than 2,000 km. Several reported localities for coesite and diamond are indicated (Modified from Zhang *et al.*, 1996). The abbreviations in Fig. 1 are described as below: SMF, Shangcheng-Macheng fault; MXF, Mozitan-Xiaotian fault; YQWF, Yantai-Qingdao-Wulian fault; GMF, Guishan-Meishan fault; XGF, Xiangfan-Guangji fault; NDU: Northern Dabie Unit; CDU: Central Dabie Unit; SDU: Southern Dabie Unit; HT: High temperature; UHP: Ultrahigh pressure; and HP: High pressure.

2. Geological setting

The NDU is dominated by upper amphibolite- and granulite-facies supracrustal sequences (~ 15 %) and orthogneisses (~ 85 %) (Wang, 1991; Wang *et al.*, 1992; Suo *et al.*, 1993; Jian *et al.*, 1997; Chen *et al.*, 1998; Wang Q. *et al.*, 2000a). Field observations at Fuzhihe (Hubei) (Fig. 2) indicate that the protoliths of orthogneisses intruded the supracrustal sequences (Wang, 1991; Suo *et al.*, 1993). Still later, post-collisional undeformed or weakly deformed mafic-ultramafic and granitic plutons intruded these two rock types (*e.g.*, Li & Wang, 1991;

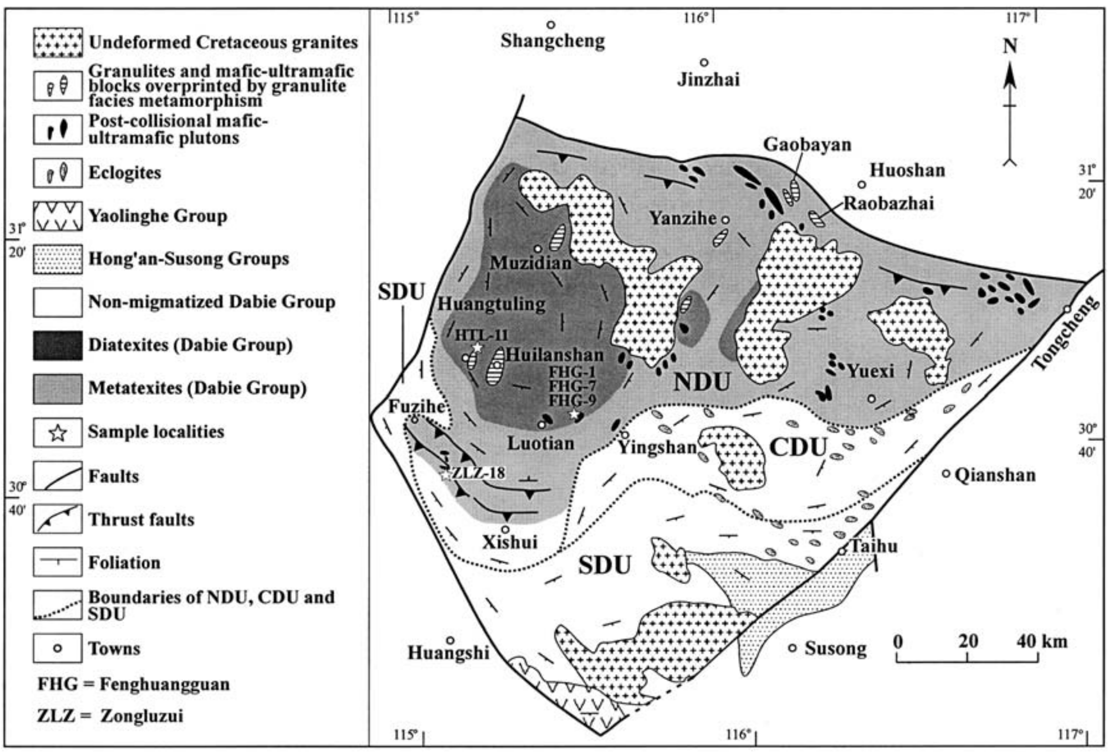

Fig. 2. Schematic geologic map of the Dabie Shan, east-central China, illustrating the sampling localities and distribution of the granulites, eclogites, diatexites, metatexites and post-collisional mafic-ultramafic-igneous plutons (modified from Wang, 1991; Wang *et al.*, 1997; Suo *et al.*, 2000). The terms of SDU, CDU and NDU represent Southern Dabie Unit, Central Dabie Unit and Northern Dabie Unit, respectively.

Table 1. Major element analyses on leucosomes, melanosomes and bulk migmatites and one granulite from Fenghuangguan, Zongluziu and Huangtuling in the NDU.

Locality	Sample	Zone	Rock type	SiO_2	TiO_2	Al_2O_3	FeO*	MnO	MgO	CaO	Na_2O	K_2O	P_2O_5	LOI	Total
Fenghuangguan	FHG-1	L	Tonalite	73.11	0.10	14.65	0.97	0.11	0.47	3.68	4.67	0.84	0.10	1.26	99.96
		Wr	Tonalite	66.51	0.59	15.15	5.38	0.15	1.68	3.47	3.57	1.12	0.14	2.23	99.99
		M	Granodiorite	55.34	1.25	16.53	8.95	0.28	3.65	2.79	2.57	2.24	0.19	6.20	99.99
	FHG-7	L	Tonalite	71.94	0.23	15.77	1.81	0.16	0.78	3.69	4.16	0.68	0.12	0.64	99.98
		Wr	Tonalite	66.21	0.39	15.98	4.98	0.20	2.12	3.27	3.68	1.33	0.24	1.57	99.97
		M	Granodiorite	61.23	0.84	16.26	7.61	0.28	3.76	2.47	2.26	2.26	0.36	2.66	99.99
	FHG-9	L	Granite	72.44	0.08	14.43	1.31	0.03	0.31	1.59	4.06	5.28	0.08	0.34	99.95
		Wr	Granodiorite	68.14	0.40	15.38	3.55	0.09	1.13	2.49	3.66	3.88	0.12	1.08	99.92
		M	Granodiorite	65.84	1.76	16.10	5.06	0.14	1.45	2.88	2.97	2.33	0.19	1.27	99.99
Zongluzui	ZLZ-18	L	Granodiorite	67.63	0.22	16.87	3.87	0.18	1.76	2.31	3.65	2.42	0.16	0.87	99.94
		Wr	Granodiorite	65.19	0.91	15.36	5.85	0.21	2.59	2.66	3.29	2.51	0.24	1.09	99.90
		M	Granodiorite	56.47	1.47	14.97	11.31	0.34	3.44	3.06	2.96	3.32	0.52	2.09	99.95
Huangtuling	HTL-11	Wr	Granulite	61.91	0.92	14.31	8.92	0.26	5.47	1.00	1.79	1.60	0.11	3.69	99.98

Notes: (1) FeO* is the total iron; (2) Oxides are in wt %; (3) Analyzed by wet chemistry; (4) The classification of rocks is based on the An-Ab-Or diagram (Baker, 1979); (5) L, leucosomes; M, melanosomes, and Wr, whole-rocks.

Hacker *et al.*, 1998; Jahn *et al.*, 1999; Li *et al.*, 1999). Large-scale multiple-phase folds are common in the supracrustal sequences (Wang, 1991; Wang *et al.*, 1992), whereas small-scale irregular folds are characteristic for the orthogneisses.

The supracrustal sequences include marble, calcsilicate rock, quartzite, metamorphosed banded iron formation, schist, amphibolite and migmatite (Wang, 1991; Suo *et al.*, 1993; Zhang *et al.*, 1996). The protoliths of these supracrustal rocks are considered to be carbonate, chert, pelite, volcanic or tuffaceous basaltic and feldspathic rocks, sandstone and greywacke (Wang, 1991; Suo *et al.*, 1993). The so-called orthogneisses comprise abundant migmatites that are particularly abundant in the western NDU (Fig. 2). The protoliths of the orthogneisses include rocks of the trondhjemite-tonalite-granodiorite suite (TTG sensu Baker, 1979). Some felsic (*e.g.*, Huangtuling) and mafic (*e.g.*, Huilanshan) granulite blocks also occur in the NDU (Fig. 2). Our field observations suggest that these isolated granulite blocks tectonically overlie the supracrustal sequences and / or orthogneisses.

The field area of this study is situated in the western NDU (Fig. 2), where the Dabie metamorphic rocks occur as a dome (named as Luotian dome) characterized by concentric foliations and abundant diatexite (sensu Mehnert, 1968) in its central part. At the outcrop scale, diatexites vary from homogeneous to heterogeneous structures with schlierens and intercalations of metatexites and restites. The central diatexites are surrounded by metatexites with variable textures (Fig. 2). Although the areal extents of diatexites and metatexites are roughly illustrated in Fig. 2, their actual boundaries are usually gradual and vague. The migmatites are overprinted by later foliation and lineation (Zhang *et al.*, 1996; Faure *et al.*, 1999), but the primary migmatitic fabric is still well recognizable. Moving to the northern and eastern margins of the Luotian dome (Fig. 2), gneissic migmatites are more and more mylonitized. The plutons of orthogneisses with TTG compositions are heterogeneously deformed and foliated with mylonitic rims around undeformed or weakly foliated cores. These orthogneissic plutons are not always distinguished from anatectic granitoids, but hectometre-scale enclaves of mylonitic migmatites in these plutons manifest that the main deformation in the NDU was completed before Cretaceous pluton emplacement.

The migmatite and granulite samples were collected at Fenghuangguan (FHG) and Zongluzui (ZLZ), near to the southern margin of the Luotian dome (Fig. 2). In these locations, most leucosomes occur as 0.5-1.0 cm thick, concordant or slightly discordant veins that are commonly folded. Some leucosomes, however, appear along extensional fractures, up to 20 cm wide. The leucosomes consist of quartz, plagiolcase, K-feldspar, biotite, hornblende and accessory minerals and range in composition from tonalite (with plagioclase of An_{35-28}) *via* granodiorite (An_{31-22}) to granite (An_{28-17}). Melanosomes are composed of biotite, hornblende, plagioclase (An_{40-28}), quartz and minor magnetite and apatite. The mesosomes are made of quartz + plagioclase (An_{45-38}) + hornblende ± biotite ± clinopyroxene and accessory minerals. Bulk-rock chemical analyses of selected samples from leucosomes, melanosomes and bulk migmatites are given in Table 1. Previous geothermobarometric studies suggest that the leucosomes were formed at P = 0.52-0.55 GPa and T = 760-820°C, corresponding to a metamorphic field gradient of *ca.* 40°C/km (Wang, 1991; Zhang *et al.*, 1996; Wang *et al.*, 1997). Most leucosomes in the NDU are considered to be the result of anatexis, but some may be originated from fluid metasomatism (Wang, 1991; Wang *et al.*, 1997).

3. Analytical procedures

Four leucosome, four melanosome, four bulk migmatite and one felsic granulite samples were chosen for chemical and isotopic analyses. Zircon, apatite, plagioclase, hornblende, biotite and K-feldspar were separated from five of the above samples, using a conventional magnetic isodynamic separator followed by heavy liquid. Final handpicking ensured a purity better than 99 %. Most zircons are

Table 2. Zircon U-Pb data for a tonalitic leucosome in the migmatites at Fenghuanguan in the NDU.

Fraction[a]	Weight (μg)	U (ppm)	Pb (ppm)	Common Pb (pg)	$^{206}Pb/^{204}Pb$[b]	$^{208}Pb/^{206}Pb$[c]	$^{206}Pb/^{238}U$[c] (± 2σ)[e]	$^{207}Pb/^{235}U$[c] (± 2σ)	$^{207}Pb/^{206}Pb$[c] (± 2σ)	$t_{206/238}$[d] (± 2σ) (Ma)	$t_{207/235}$[d] (Ma)	$t_{207/206}$[d] (Ma)
1	40	273.5	5.381	4.5	1851	0.09051	0.01938(21)	0.134(22)	0.0503(78)	123.7±1.4	128±22	207±32
2	30	163.2	4.564	22	190	0.08873	0.02071(23)	0.139(24)	0.0487(80)	132.1±1.5	132±24	133±22
3	40	91.23	2.842	25	156	0.1348	0.02102(26)	0.146(29)	0.0505(93)	134.1±1.7	138±29	217±40
4	35	185.5	4.256	11	486	0.08771	0.02056(14)	0.146(14)	0.0489(49)	131.2±0.9	138±14	143±14
5	35	159.6	3.821	15	398	0.09931	0.02088(21)	0.152(12)	0.0491(38)	133.2±1.4	144±12	153±12
6	40	267.2	5.875	6.9	655	0.09722	0.02078(24)	0.148(07)	0.0501(23)	132.6±1.5	140±07	200±09
7	45	226.2	4.717	5.3	1027	0.07825	0.02032(17)	0.139(05)	0.0487(19)	129.7±1.1	132±05	133±05
8	35	197.9	4.157	4.9	1234	0.07933	0.02056(19)	0.141(06)	0.0489(21)	131.2±1.2	134±06	143±06
9	45	234.3	4.983	6.1	889	0.07924	0.02036(20)	0.137(08)	0.0487(32)	129.9±1.3	130±08	133±09
10	25	158.6	3.522	7.9	599	0.08945	0.02067(23)	0.142(08)	0.0488(33)	131.9±1.5	135±08	138±09
11	25	262.5	9.753	43	169	0.1082	0.02614(23)	0.194(23)	0.0539(59)	166.3±1.5	180±23	365±40
12	25	178.6	4.755	7.3	620	0.1048	0.02532(15)	0.174(11)	0.0498(29)	161.2±1.0	163±11	184±11

[a] 1-10: Colorless, euhedral and elongate, and 11-12: light brown, subhedral and stubby. [b] Measured values, only corrected for mass fractionation. [c] Radiogenic ratios, corrected for mass fractionation, analytical Pb and U blanks, and initial common Pb. Initial Pb compositions are estimated from Stacey & Kramers (1975). [d] Calculated ages from the radiogenic ratios using the Isoplot program of Ludwig (1992), $\lambda_{238} = 1.55125\times10^{-10}\,a^{-1}$ and $\lambda_{235} = 9.8485\times10^{-10}\,a^{-1}$ (Steiger & J ger, 1977). [e] Numbers in parentheses are the 2-σ errors, *e.g.*, 0.01938(21) means 0.01938 ± 0.00021 (2σ).

Table 3. The Sm-Nd isotopic compositions for one tonalitic leucosome (FHG-1), one granodioritic leucosome (ZLZ-18) and one melanosome (FHG-1) at Fenghuangguan and Zongluzui in the NDU.

Sample	Fraction	Sm (ppm)	Nd (ppm)	$^{147}Sm/^{144}Nd$	$^{143}Nd/^{144}Nd$ (±2σ)	$\varepsilon_{Nd}(T)$ (130 Ma)	T_{DM} (Ga)	T_{2DM} (Ga)
ZLZ-18	Hb	12.20	37.46	0.1967	0.511332 (16)			
	Pl	0.6872	3.500	0.1187	0.511115 (20)			
	Bi	5.309	28.36	0.1131	0.511149 (12)			
	Wr	10.12	41.16	0.1485	0.511201 (17)	-27.2	4.50	3.13
FHG-1	Pl	0.4923	2.499	0.1191	0.512039 (16)			
	Ap	23.43	45.45	0.3116	0.512451 (25)			
	Bi	4.399	25.05	0.1061	0.511934 (27)			
	Wr-L	0.8721	4.539	0.1160	0.512044 (23)	-10.3	1.73	
	Wr-M	4.404	20.39	0.1305	0.512079 (16)	-9.8	1.96	1.72

Notes: (1) Bi, biotite; Hb, hornblende; Ap, apatite; Pl, plagioclase; Wr-L, wholerock leucosome; Wr-M, wholerock melanosome; and Wr, bulk migmatites. (2) The ratios of $^{143}Nd/^{144}Nd$ were further adjusted to the La Jolla standard = 0.511860. (3) Depleted mantle model ages (T_{DM} and T_{2DM}) related to a depleted mantle reservoir with present-day $^{147}Sm/^{144}Nd$ = 0.2137 and $^{143}Nd/^{144}Nd$ = 0.51315 for single stage and two stages were calculated after DePaolo (1988) and Zhu *et al.* (1998), respectively.

Table 4. The Rb-Sr isotopic compositions for one tonalitic leucosome (FHG-1), one granodioritic leucosome (ZLZ-18) and one melanosome (FHG-1) at Fenghuangguan and Zongluzui in the NDU.

Sample	Fraction	Rb (ppm)	Sr (ppm)	$^{87}Rb/^{86}Sr$	$^{87}Sr/^{86}Sr$ (±2σ)	$(^{87}Sr/^{86}Sr)_{130\ Ma}$	T_{CHUR}^{Sr}
FHG-1	Pl	3.82	762.4	0.0145	0.705823(16)		
	Ap	0.478	200.9	0.00686	0.705811(15)		
	Bi	285.3	16.59	50.0	0.787771(23)		
	Wr-L	7.12	466.4	0.0440	0.705913(13)	0.70583	-
	Wr-M	104.6	367.8	0.820	0.707138(12)	0.70562	304
ZLZ-18	Wr-L	71.71	393.7	0.546	0.708095(15)	0.70709	621

Notes: (1) Pl, plagioclase; Ap, apatite; Bi, biotite; Wr-L, wholerock leucosome; Wr-M, wholerock melanosome; and Wr, bulk migmatite. (2) The ratios of $^{87}Sr/^{86}Sr$ were corrected for mass fractionation relative to $^{86}Sr/^{88}Sr$ = 0.1194, and adjusted to the NBS-987 Sr Standard = 0.710250. (3) The CHUR (chondritic uniform reservoir) isotopic compositions for the calculation of Sr model ages: $^{87}Rb/^{86}Sr$ = 0.0736; $^{87}Sr/^{86}Sr$ = 0.70391 (Ludwig, 1992).

colorless, euhedral and elongated. A small proportion of zircon crystals are light brown, subhedral and stubby. All zircons chosen for analysis were clear, inclusion- and fracture-free, and devoid of visible cores under optical microscope. Zircon grains were dissolved, and U and Pb were extracted using the method of Krogh (1973, 1978). Pb and U isotopic ratios were measured on a VG 354 mass spectrometer at the Tianjin Institute of Geology and Mineral Resources. Total Pb blanks ranged from 15 to 50 pg, and total U blanks were less than 2 pg. The U-Pb isotopic data are presented in Table 2. Since these zircons are very young, the radiogenic product of ^{207}Pb is consequently

Table 5. Argon isotopic compositions for four leucosomes (ZLZ-18, FHG-1, FHG-7 and FHG-9) at Zongluzui and Fenghuangguan and a felsic granulite (HTL-11) at Huangtuling in the NDU.

Stage	Temperature (°C)	$^{40}Ar/^{39}Ar$	$^{38}Ar/^{39}Ar$	$^{37}Ar/^{39}Ar$	$^{36}Ar/^{39}Ar$	moles ^{39}Ar	%^{39}Ar Released	%^{40}Ar*#	$^{40}Ar^*/^{39}Ar_K$	Apparent age ($\pm\sigma$)(Ma)
HTL-11: Biotite, Weight = 60 mg, J = 0.013802										
1	360	394.9	4.50E-01	6.00E-01	9.35E-01	2.80 E-13	0.78	24.12	95.24	1514.8 ± 14.5
2	520	146.6	2.94E-01	3.19E-01	4.32E-01	2.14 E-13	1.38	5.51	8.09	191.1 ± 12.6
3	680	29.75	4.22E-02	1.37E-02	6.75E-02	4.05 E-12	12.71	27.25	8.12	191.4 ± 2.2
4	810	8.422	2.93E-02	4.00E-02	6.00E-04	1.15 E-11	44.80	97.76	8.24	194.2 ± 0.8
5	930	10.59	2.44E-02	4.54E-02	7.10E-03	7.14 E-12	64.82	78.30	8.30	195.5 ± 1.1
6	1030	9.223	2.01E-02	3.46E-02	2.80E-03	1.13 E-11	96.30	90.14	8.31	195.9 ± 0.7
7	1130	25.26	4.19E-01	4.49E-01	5.28E-02	4.94 E-13	97.68	32.92	8.32	196.1 ± 2.6
8	1240	22.50	2.72E-01	3.83E-01	4.39E-02	4.84 E-13	99.03	37.50	8.43	198.7 ± 3.1
9	1340	28.19	1.59E-01	1.87E-01	6.23E-02	3.46 E-13	100.00	29.14	8.22	193.8 ± 8.2
ZLZ-18: Hornblende, Weight = 140 mg, J = 0.013677										
1	750	22.68	4.27E-01	7.22E-01	4.75 E-03	3.78 E-14	2.25	93.81	21.27	434.0 ± 3.1
2	900	5.722	2.07E-01	1.32E+00	1.46 E-03	2.95 E-12	19.80	92.46	5.29	116.2 ± 1.0
3	1030	5.632	1.88E-01	1.21E+00	1.46 E-03	3.44 E-12	40.30	92.34	5.20	114.0 ± 0.9
4	1130	5.171	2.08E-01	1.54E+00	9.74 E-04	8.83 E-12	92.92	94.43	4.88	110.0 ± 0.4
5	1240	6.873	2.33E-01	1.63E+00	3.77 E-03	1.14 E-13	99.71	83.76	5.75	111.2 ± 2.3
6	1340	254.2	4.38E-01	1.91E+00	8.39 E-01	4.91 E-14	100.00	2.43	6.19	161.0 ± 44.3
FHG-1: Biotite, Weight = 5.16 mg , J = 0.006975										
1	600	12.82	3.37E+00	4.85E-02	2.06E-02	3.88E-14	5.04	52.40	6.73	82.7 ± 3.0
2	700	9.531	7.27E-02	7.51E-03	2.45E-03	1.06E-13	18.80	92.10	8.78	107.3 ± 0.2
3	780	9.656	2.34E-02	1.16E-02	3.34E-03	7.96E-14	29.10	89.40	8.65	105.6 ± 0.4
4	850	9.628	2.32E-02	1.04E-02	2.83E-03	6.63E-14	37.70	90.90	8.77	107.1 ± 0.5
5	950	9.229	2.14E-02	4.94E-03	1.54E-03	1.28E-13	54.30	94.70	8.75	106.9 ± 0.3
6	1100	8.962	2.06E-02	2.80E-03	7.39E-04	3.51E-13	100.00	97.30	8.72	106.5 ± 0.4
FHG-7: K-feldspar, Weight = 6.01 mg , J = 0.006972										
1	600	19.83	7.52E-01	1.77E-02	1.32E-02	6.86E-14	6.92	80.20	15.92	189.9 ± 0.7
2	700	9.519	2.95E-02	5.08E-02	6.72E-03	8.51E-14	15.50	78.80	7.51	92.1 ± 1.8
3	800	8.914	2.41E-02	-3.79E-02	7.42E-03	7.04E-14	22.60	74.90	6.69	82.3 ± 4.4
4	850	9.755	1.85E-02	1.84E-02	7.85E-03	1.16E-14	23.80	75.20	7.41	90.9 ± 1.6
5	950	10.08	1.82E-02	1.90E-02	8.97E-03	4.40E-14	28.20	73.30	7.40	90.8 ± 0.9
6	1000	9.671	1.69E-02	1.39E-02	7.23E-03	5.02E-14	33.30	77.50	7.51	92.1 ± 0.7
7	1100	9.216	1.97E-02	3.39E-02	5.75E-03	5.56E-15	33.80	79.50	7.49	91.9 ± 2.8
8	1200	9.389	1.66E-02	2.05E-02	6.12E-03	3.08E-14	36.90	80.20	7.56	92.7 ± 0.7
9	1300	9.058	1.28E-02	4.78E-03	1.97E-03	6.25E-13	100.00	93.30	8.45	103.3 ± 0.1
FHG-9: Hornbelnde, Weight = 22.41 mg, J = 0.006961										
1	750	38.69	7.06E-01	2.37E+00	7.90E-02	4.57E-15	3.55	39.80	15.52	185.1 ± 7.8
2	850	28.54	5.01E-02	3.47E+00	6.11E-02	5.32E-15	7.68	37.40	10.76	130.3 ± 3.5
3	950	24.90	8.35E-02	4.98E+00	5.19E-02	8.14E-15	14.00	39.60	9.94	120.7 ± 5.5
4	980	17.57	8.78E-02	5.67E+00	2.66E-02	7.24E-15	19.60	57.10	10.15	123.2 ± 4.0
5	1010	12.74	8.23E-02	5.56E+00	1.32E-02	2.51E-14	39.10	72.30	9.27	112.8 ± 1.3
6	1030	12.21	8.00E-02	5.57E+00	1.03E-02	4.42E-14	73.40	78.00	9.58	116.5 ± 1.0
7	1200	14.78	7.90E-02	5.16E+00	1.82E-02	2.33E-14	91.50	65.80	9.79	118.9 ± 1.0
8	1350	17.88	8.01E-02	5.53E+00	3.17E-02	1.09E-14	100.00	49.50	8.93	108.8 ± 2.8

Notes: (1) ^{40}Ar* represents the radiogenic argon. (2) Uncertainties of ^{40}Ar* and $^{39}Ar_K$ are less than 3% for the sample FHG-1, FHG-7 and FHG-9, and ± 5% for the sample HTL-11 and ZLZ-18. (3) The errors of J-factor measurements are not included in those of apparent ages.

extremely low, the errors for $^{207}Pb/^{235}U$ and $^{207}Pb/^{206}Pb$ ratios are evidently higher than that for $^{206}Pb/^{238}U$, and $^{207}Pb/^{206}Pb$ ages can be erroneously high. We also note that the large errors for $^{207}Pb/^{235}U$ and $^{207}Pb/^{206}Pb$ arise for those samples with high common Pb (*e.g.*, fractions 2, 3 and 11). Therefore, we use the $^{206}Pb/^{238}U$ ages in our discussion.

Fresh chips of leucosomes, melanosomes, and bulk migmatites*,* as well as pure mineral separates, were washed with deionized water in an ultrasonic bath. After drying, the samples were pulverized to about 200 mesh using a hardened steel mortar and pestle. These sample powders were used for major element and Rb-Sr and Sm-Nd isotope analyses. Major elements were analyzed using conventional wet chemistry method for the leucosome, melanosome and bulk migmatite, and data are presented in Table 1. Rb-Sr and Sm-Nd analytical procedures were described by Wang *et al.* (2001). Rb, Sr, Sm and Nd isotope analyses were performed on a VG 354 mass spectrometer at the Guangzhou Institute of Geochemistry, Chinese Academy of Sciences (GIG-

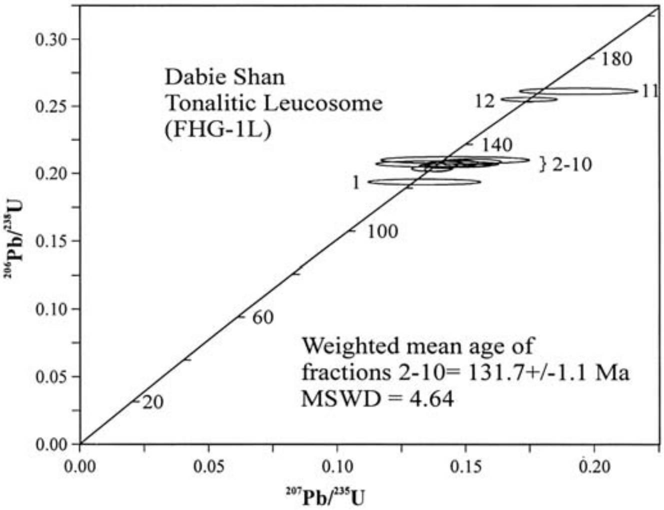

Fig. 3. Concordia diagram showing the zircon U-Pb data for a tonalitic leucosome at Fenghuangguan in the NDU.

CAS). $^{87}Sr/^{86}Sr$ and $^{143}Nd/^{144}Nd$ ratios were normalized to $^{86}Sr/^{88}Sr$ = 0.1194 and $^{146}Nd/^{144}Nd$ = 0.7219, respectively. During the course of this study, NBS-987 gave an average $^{87}Sr/^{86}Sr$ ratio of 0.710242 ± 12 (2σ); La Jolla standard gave a mean $^{143}Nd/^{144}Nd$ ratio of 0.511861 ± 16 (2σ). The Sm-Nd and Rb-Sr isotopic data are presented in Tables 3 and 4. Sm-Nd and Rb-Sr isochron calculations were performed using the Isoplot program (Ludwig, 1992). Input errors for age computations are $^{147}Sm/^{144}Nd$ = 0.2 %, $^{143}Nd/^{144}Nd$ = 0.005 %, $^{87}Rb/^{86}Sr$ = 2 % and $^{87}Sr/^{86}Sr$ = 0.005 %.

Ar isotopic analyses were conducted partly at GIG-CAS and partly at UCLA. A biotite separate from sample ZLZ-18 and a hornblende separate from sample HTL-11 were wrapped in aluminum foil and irradiated in Reactor 902 in Mianyang (Sichuan), together with a biotite standard (ZBH-2506) with a known age of 132.7 ± 1.2 Ma. Argon isotope compositions were analyzed on a MM-1200 mass spectrometer at GIG-CAS. Step-heating was carried out incrementally after 24 hours pre-heating, and each step lasted 30 minutes (see Dai & Hong, 1982). Another hornblende separate from sample FHG-9, another biotite separate from sample FHG-1 and a K-feldspar separate from sample FHG-7 were wrapped in aluminum foil and irradiated in the Ford Reactor, University of Michigan, together with the Fish Canyon sanidine (FC-3) monitor standard with a known age of 27.8 ± 0.3 Ma. *J*-factors were determined by the laser ablation technique. The irradiated samples were step-heated in a tantalum crucible within a double-vacuum furnace and analyzed with a VG 3600 mass spectrometer at the University of California, Los Angeles (UCLA). $^{40}Ar/^{39}Ar$ ages were calculated using the constants recommended by Steiger & Jäger (1977). All errors are quoted at the 1-sigma level and do not include the uncertainty of the monitor age. Argon blanks over the course of these analyses averaged 2-5 × 10^{-16} mole ^{40}Ar with an atmospheric ratio. The detailed experimental procedure was described by Harrison *et al.* (1996). The Ar isotopic compositions are presented in Table 5.

4. Results

4.1 Zircon U-Pb system

The U-Pb data of twelve zircon fractions from one tonalitic leucosome (FHG-1L) at Fenghuangguan (Table 2) are plotted in the concordia diagram (Fig. 3). All of them yield concordant ages. Fraction 1 yields a $^{206}Pb/^{238}U$ age of 123.7 ± 1.4 Ma, fractions 2-10 give a weighted mean $^{206}Pb/^{238}U$ age of 131.7 ± 1.1 Ma with MSWD = 4.64 and fractions 11-12 define an average $^{206}Pb/^{238}U$ age of 163.8 ± 1.3 Ma.

4.2 Sm-Nd system

Single stage depleted mantle model ages (T_{DM}) were calculated from the Sm-Nd isotopic data using the following equation (DePaolo, 1988):

$$T_{DM} = 1/\lambda_{sm} \ln[1 + (^{143}Nd/^{144}Nd - 0.51315) / (^{147}Sm/^{144}Nd - 0.2137)] \quad (1).$$

For the samples with $^{147}Sm/^{144}Nd$ > 0.13 or < 0.10, two-stage Nd model ages (T_{2DM}) were also calculated in order to see the bias of T_{DM} caused by significant Sm/Nd fractionation (Zhu *et al.*, 1998):

$$T_{2DM} = 1/\lambda_{sm} \ln\{1 + [0.51315 - {}^{143}Nd/^{144}Nd + (^{147}Sm/^{144}Nd - 0.118)(e^{\lambda_{sm} t} - 1)]/(0.2137 - 0.118)\} \quad (2),$$

where *t* is the assumed age of migmatization (132 Ma), and 0.118 is the assumed average $^{147}Sm/^{144}Nd$ ratio of the continental crust.

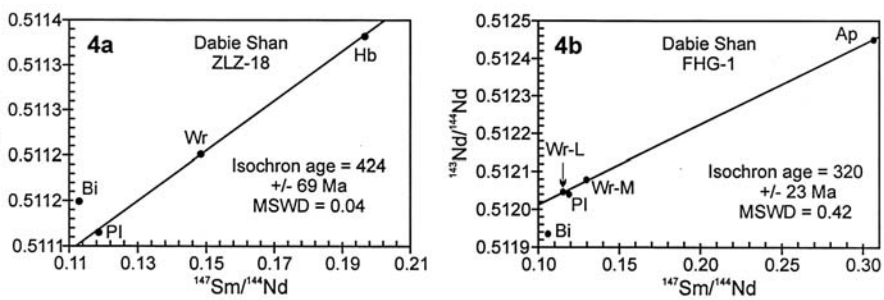

Fig. 4. Sm-Nd internal isochron diagrams for mineral separates and whole-rocks from one granodioritic migmatite (ZLZ-18) at Zongluzui (4a) and one tonalitic migmatite (FHG-1) at Fenghuangguan (4b) in the NDU.

The $^{147}Sm/^{144}Nd$ ratios for hornblende, biotite, plagioclase mineral separates and the wholerock sample of granodioritic leucosome ZLZ-18 vary from 0.1131 to 0.1967 (Table 3). Hornblende, plagioclase and wholerock sample fall on a linear line on the Sm-Nd isochron diagram, corresponding to an age of 424 ± 69 Ma with MSWD = 0.04 (Fig. 4a). The whole rock yields an initial ε_{Nd}-value of –27.2 at 130 Ma, and Nd model ages of 4.50 Ga (T_{DM}) and 3.13 Ga (T_{2DM}). The $^{147}Sm/^{144}Nd$ ratios for biotite, plagioclase, apatite mineral separates, one leucosome and one melanosome sample from the tonalitic migmatite FHG-1 range from 0.1061 to 0.3116 (Table 3). The two wholerock samples (melanosome and leucosome) and the plagioclase and apatite mineral separates define a linear line in Sm-Nd isochron diagram, corresponding to an age of 320 ± 23 Ma with MSWD = 0.42 (Fig. 4b). The leucosome and melanosome give initial ε_{Nd}-values of –10.3 and –9.8, respectively, at 130 Ma (zircon U-Pb age). The Nd model ages are 1.73 Ga and 1.72 Ga for the leucosome (T_{DM}) and melanosome (T_{2DM}), respectively (Table 3).

4.3 Rb-Sr system

One leucosome, one melanosome and three mineral separates (apatite, biotite and plagioclase) from the tonalitic leucosome (FHG-1), defined a linear line in the Rb-Sr isochron diagram, corresponding to an age of 115 ± 2 Ma with an initial $^{87}Sr/^{86}Sr$ ratio of 0.70581, with a MSWD value of 1.4 (Table 5 and Fig. 5). The line is largely controlled by biotite, plagioclase and apatite deviate slightly from the line. The leucosome and melanosome samples give initial $^{87}Sr/^{86}Sr$ ratios of 0.70584 and 0.70562, respectively at 130 Ma. A granodioritic migmatite (ZLZ-18) was also analyzed for its whole rock Rb-Sr isotopic composition (Table 4). This sample yields an initial $^{87}Sr/^{86}Sr$ ratios of 0.70709 at 130 Ma.

4.4 $^{40}Ar/^{39}Ar$ system

The hornblende separate from a leucosome collected from Zongluzui (ZLZ-18), the hornlende, biotite and K-feldspar separates (FHG-9, FHG-1 and FHG-7, respectively) from a leucosome collected from Fenghuangguan, and the biotite separate from a felsic granulite (HTL-11) collected from Huangtuling were analysed for Ar isotope compositions (Table 5). Data of steps 2-5 for the hornblende separate (sample ZLZ-18) form a linear line in Ar-Ar isochron diagram, corresponding to an age of 114 ± 1 Ma, with an initial $^{40}Ar/^{36}Ar$ ratio of 588 ± 12 (Fig. 6A). These steps released 97.5 % of the total ^{39}Ar, and give a main plateau age of 112 ± 2 Ma (Fig. 6B). Data for the other hornblende separate (sample FHG-9) form a linear line in Ar-Ar isochron plot, corresponding to an age of 111.1 ± 1.1 Ma, with an initial $^{40}Ar/^{36}Ar$ ratio of 329 ± 5 (Fig. 6C). The steps 3-8 of this sample released 92.3 % of the total ^{39}Ar, and give a plateau age of 116.2 ± 1.7 Ma (Fig. 6D). Data for the biotite separate (sample FHG-1) cluster around a line in Ar-Ar isochron diagram, except for the first step, corresponding to an age of 106.7 ± 0.5 Ma with an initial $^{40}Ar/^{36}Ar$ of 302 ± 16 (Fig. 6E). These steps

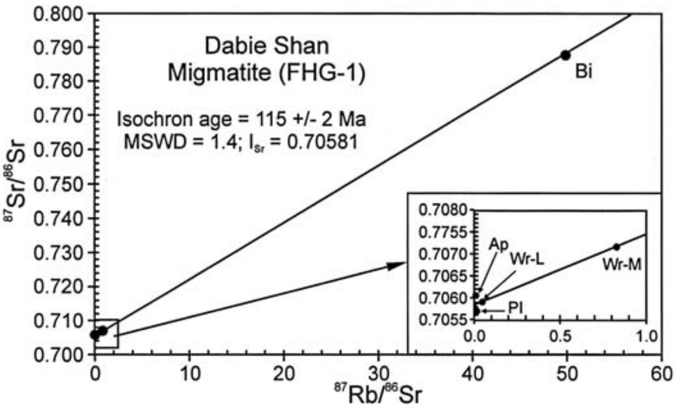

Fig. 5. Rb-Sr internal isochron diagram of mineral separates and whole-rock samples from one tonalitic migmatites (FHG-1) at Fenghuangguan in the NDU.

release 95.0 % of the total ^{39}Ar, and give a plateau age of 106.7 ± 0.6 Ma (Fig. 6F). Data for the K-feldspar separate from sample FHG-7 cluster around a linear line in Ar-Ar isochron diagram, corresponding to an age of 95.3 ± 2.3 Ma with an initial $^{40}Ar/^{36}Ar$ of 255 ± 27 (Fig. 6G). The steps 2-9 release 93.1 % of the total ^{39}Ar, corresponds to a plateau age of 98.8 ± 0.8 Ma (Fig. 6H). Data for the biotite separate from one felsic granulite (HTL-11) give an isochron of 194 ± 2 Ma with an initial $^{40}Ar/^{36}Ar$ of 321 ± 3 (Fig. 6I). The steps 3-8 released 97.7 % of the total ^{39}Ar, and yield a plateau age of 195 ± 2 Ma (Fig. 6J).

5. Discussion

5.1 Age of granulite-facies metamorphism

Granulites are exposed in several localities in the NDU (Fig. 2). Field investigations suggest that the isolated granulite blocks tectonically overlie the supracrustal sequences and/or orthogneisses *via* thrusting. We propose that the granulites in the NDU are exotic blocks, probably as scraps from the CDU and / or SDU. This proposal is consistent with the fact that the boundary between the granulite blocks and migmatized supracrustal sequences and / or orthogneisses are always bounded by faults. The biotite separate from the felsic granulite at Huangtuling (Fig. 2) gives 195 ± 2 Ma $^{40}Ar/^{39}Ar$ plateau and 194 ± 2 Ma isochron ages (Fig. 6I and 6J), indicating that the granulite was cooled to below ~ 350°C at 195 Ma. These felsic granulites show well-preserved garnet growth zoning, suggesting that peak metamorphic conditions were not maintained for a long period of time (Chen *et al.*, 1998). Thus, we consider that the 195 Ma age records the rapid uplift of the granulite shortly after the peak metamorphism. Therefore the minimum age of grnulite-facies metamorphism is ~ 195 Ma. This conclusion is consistent with the recent geochronological study of granulites from Laobazhai and Gaobayan (Fig. 2), which suggests that the granulite-facies metamorphism shortly followed the 210-230 Ma UHP metamorphism (Li *et al.*, 1993).

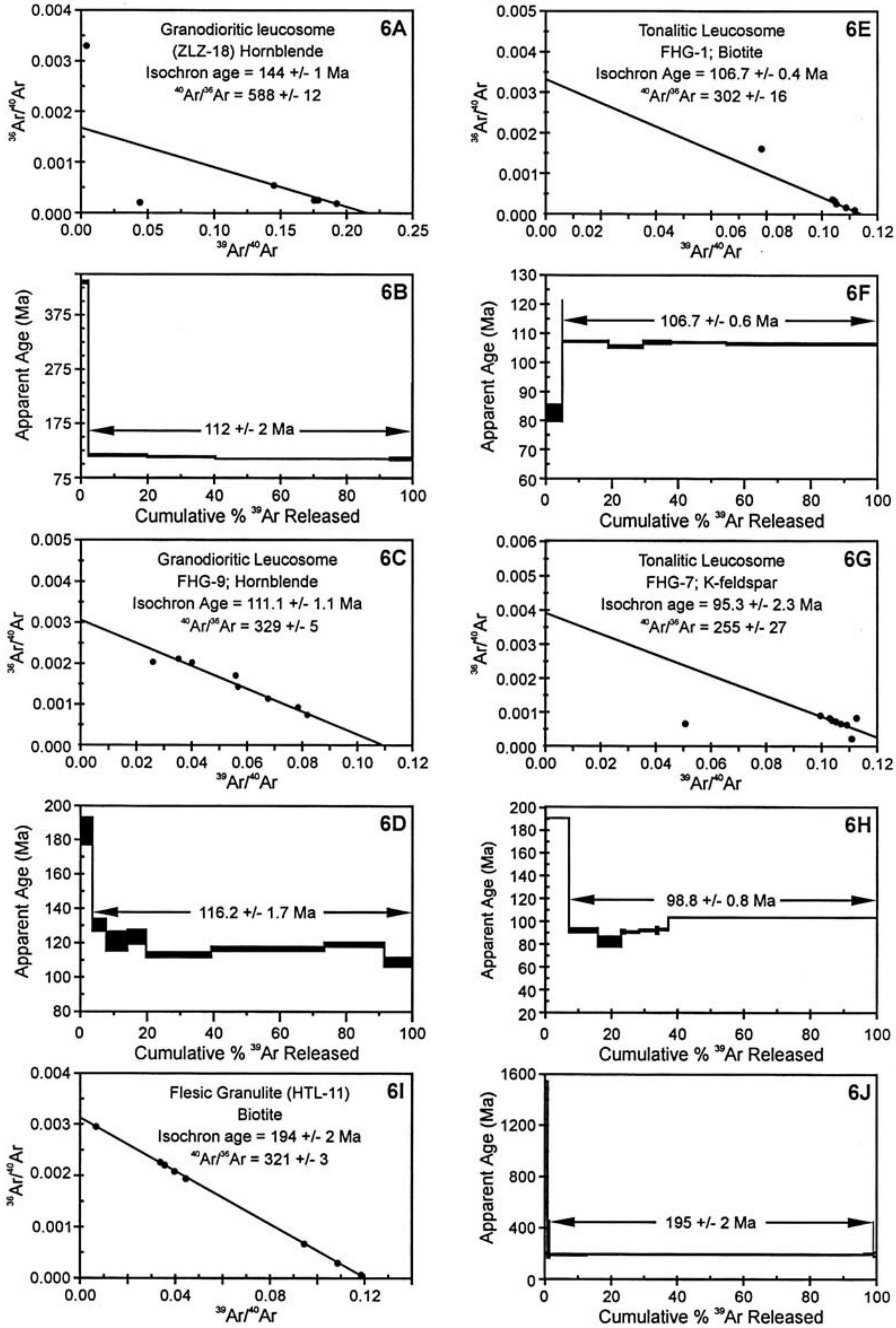

Fig. 6. $^{40}Ar/^{39}Ar$ isochron and plateau ages for four leucosomes from migmatites and one granulite in the NDU. 6A and 6B, Hornblende $^{40}Ar/^{39}Ar$ isochron and plateau ages for a granodioritic leucosome at Zongluzui (ZLZ-18). 6C and 6D, Hornblende $^{40}Ar/^{39}Ar$ isochron and plateau ages for a tonalitic leucosome at Fenghuangguan (FHG-9). 6E and 6F, Biotite $^{40}Ar/^{39}Ar$ isochron and plateau ages for a tonalitic leucosome at Fenghuangguan (FHG-1). 6G and 6H, K-feldspar $^{40}Ar/^{39}Ar$ isochron and plateau ages for a granitic leucosome at Fenghuangguan (FHG-7). 6I and 6J, Biotite $^{40}Ar/^{39}Ar$ isochron and plateau ages for a granulite at Huangtuling (HTL-11). The errors for plateau ages do not include the analytical errors of J-factors.

5.2 Geochronological constraints on HT rocks and their protoliths

There is a general consensus that the peak HP-UHP metamorphism in the CDU and SDU happened between 210 to 230 Ma (Liou *et al.*, 1996). However, hot debates exist on the timing of HT metamorphism in the NDU. Suo *et al*. (1993) suggested that multiple phases of migmatization occurred in the NDU and Tongbai Shan (west to the NDU) from Precambrian to Mesozoic time. Zhang *et al*. (1996) proposed that the migmatization may be coeval with or shortly after the UHP metamorphism, on the basis of previously published Sm-Nd isochron ages of 220-244 Ma (Li *et al*., 1993) and the intrusive relationship of Cretaceous granitic plutons into the migmatites.

Xue *et al*. (1997) derived a zircon U-Pb age of 134 ± 2 Ma for a granitic orthogneisses and a zircon U-Pb age of 125.6 ± 0.3 Ma for an undeformed granodioritic pluton from the NDU. Hacker *et al*. (1998) reported the SHRIMP zircon ages of 129 ± 2 Ma for a weakly deformed gabbro, 138 ± 6 to 131 ± 2 Ma (zircon rims) for tonalitic orthogneisses, 134 ± 3 Ma for a weakly deformed tonalite and 130 ± 3 Ma for an undeformed granites in the NDU. Based on these data, Hacker *et al*. (1998) proposed that the NDU is actually a Cretaceous magmatic complex without a pre-Cretaceous basement, the pre-Cretaceous granulites and minor marble and ultramafic rocks are only scraps of the Yangtze Craton that survived in deep subduction. These authors argued that the term "migmatite" in the NDU was in many cases used for strongly deformed plutons, and that the crystallization pressure of weakly deformed plutons (*ca.* 0.5 GPa) are the same as those inferred for amphibolite-facies metamorphism (Zhang *et al.*, 1996) and migmatization (0.52-0.55 GPa, Wang, 1991; Wang *et al.*, 1997). Therefore, the NDU actually underwent an amphibolite-facies metamorphism, which can be defined by the 131-138 Ma zircon rim ages for the tonalitic orthogneiss (Hacker *et al.*, 1998). Our zircon U-Pb age of 131.7 ± 1.1 Ma for the leucosome of the migmatite in the NDU is consistent with the above mentioned previous data. The inherited zircons older than 164 Ma are not detected in this study. Therefore our zircon data support the above magmatic complex proposal.

However, if the NDU was indeed a Cretaceous magmatic complex (Hacker *et al.,* 1998), then an immediate question will follow: what are the source materials for the voluminous igneous rocks after the collision of the Yangtze Craton with the Sino-Korean Craton? These igneous / gneissic rocks have TTG compositions with arc signatures (Zheng *et al.*, 1999, 2000; Wang Q. *et al.*, 2000b), which generally require melting of relatively young and hot subducted slabs in the source region (Defant & Drummond, 1990; Martin, 1999), but the subduction process between the Yangtze and Sino-Korean Cratons ceased long time before this thermal activity.

Our Sm-Nd isotopic data, however, demonstrate the existence of old materials in the source of migmatites. All wholerock samples for the migmatite, leucosome and melanosome have very low negative ε_{Nd} values at 130 Ma, and give Precambrian model ages. Zhou *et al.* (1995) derived five zircon ages of 600-800 Ma for granitic gneisses from the NDU and Beihuaiyang belt. We note that Hacker *et al*. (1998) also reported SHRIMP zircon ages of 771 ± 28 to 768 ± 31 Ma for zircon cores from two tonalitic orthogneisses in the NDU, although these old zircons were interpreted as scraps of the Yangtze Craton (Hacker *et al.,* 1998). More recently, Chen *et al.* (2000) obtained 230 to 718 Ma zircon U-Pb ages for two deformed gneisses from Lutushi and Daoshichong in the NDU employing the SIMS technique. Zheng *et al.* (2000) reported a wholerock Sm-Nd isochron age of 1047 ± 45 Ma for the deformed gray gneisses in the NDU. Therefore, we consider that although the pre-Cretaceous granulites and associate supracrustal rocks were originally away from the NDU, the NDU still consists of Pre-Cretaceous rocks, such as these Precambrian orthogneisses. This unit underwent thermal event at ~ 132 Ma, *i.e.* after continental collision, resulting in migmatization and intrusion of some granitic plutons. Our study did not define the timing for amphibolite-facies metamorphism, but this may be also a result of this thermal activity.

5.3 Cooling history of the HT rocks

If we accept the cooling age concept and closure temperatures (500°C for hornblende and 350°C for biotite), the Rb-Sr age for biotite should be younger than the $^{40}Ar/^{39}Ar$ age for hornblende. In this case, the Rb-Sr age of 115 ± 2 Ma for biotite is slightly older than or close to the $^{40}Ar/^{39}Ar$ age for hornblende. Theoretically, we could lower the Rb-Sr age for biotite and increase the $^{40}Ar/^{39}Ar$ age for hornblende by playing around with the errors. Coupled with the field observations, decoupling between the Rb-Sr age for biotite and $^{40}Ar/^{39}Ar$ age for hornblende may result from hornblende recrystallization induced by a fluid activity. There were certainly huge amounts of fluids circulating in the migmatites after extensive plutonism, which may have disturbed the isotopic systems. The mechanism of fluids inducing recrystallization would also explain a lead loss of zircons (*i.e.*, 123.7 ± 1.4 Ma U-Pb age). Thus, the $^{40}Ar/^{39}Ar$ of 114 Ma for hornblende may just record the time of a fluid activity below 350°C. Obviously, the migmatization in the NDU is later than the granulite-facies and HP-UHP metamorphism.

Field observations indicate that hornblende in leucosomes and melanosomes was recrystallized and locally became megacrysts with size up to 4 mm × 12 mm. Ar isotopic results of this study can be used to constrain the cooling history of the NDU after the 132 Ma migmatization. Since different minerals have different closure temperatures for isotopic systems, the 132 Ma U-Pb zircon age, the 111-114 Ma, 107 Ma and 95 Ma $^{40}Ar/^{39}Ar$ age for the recrystalized hornblende, biotite and feldspar, respectively, can be used to study the cooling history of the migmatite and therefore the whole NDU. Combined with the closure temperatures for the above isotopic systems (McDougall & Harrison, 1999; Geyh & Schleicher, 1990), two cooling rates of 12°C/Ma and 10°C/Ma corresponding to two temperature intervals of 650-350°C and 350-230°C can be estimated for the migmatites. The low cooling rate (at least one magnitude less) of the migmatite is in sharp contrast with the rapid cooling rate of the granulite (Chen *et al.*, 1998), indicating different cooling history and different cooling magnitude for the two rock types, and therefore for different units in the study area.

6. Geodynamic implications

According to Jahn *et al.* (1999), the heat necessary for the formation of the Cretaceous migmatites could have been provided by (a) underplating of a small plume at shallow depth or (b) a combination of heat produced by radioactive decay in the thickened crust after collision and by asthenospheric upwelling during post-collisional extension. We consider the heat for migmatization in NDU is related to disturbance of the lithospheric root after the continental collision in the region. The Yangtze Craton was subducted northwards into the mantle to > 50-km depth underneath the North China Craton in the Triassic time. Small amount of water was stored in high-Si muscovite, omphacite and rutile minerals (Zhang *et al.*, 2000). Due to its buoyancy, the upper-part of the lithosphere ceased to descend, while the dense eclogitic lithosphere broke off from it and continued its descent. Because the subducted crust was cold and has a low water content, extensive partial melting and regional migmatization did not occur immediately after collision (Liou *et al.*, 1996; Jahn *et al.*, 1999).

Subsequent thermal perturbation may induce widespread partial melting of lithospheric materials due to lithospheric root removal or magmatic underplating. An influx of hot asthenospheric mantle may provide thermal energy to melt subcontinental lithospheric mantle and the base of the crust. This hypothesis is supported by the existence of 159-120 Ma post-tectonic mafic-ultramafic intrusions into the NDU (Fig. 2; Ge *et al.*, 1999; Jahn *et al.*, 1999; Chen *et al.*, 2001). Geochemical and isotopic data demonstrated that these mafic-ultramafic rocks were generated by melting of metasomatized subcontinental mantle, a result of crust-mantle interaction (Jahn *et al.*, 1999). The emplacement of mantle-derived magmas into the lower crust resulted in crustal melting and regional migmatization. There is a firm evidence that the lithospheric mantle under east China underwent a dramatic change in its thermal state in Mesozoic time, from a thick (180-200 km) and cold (40 mW/m^2) lithosphere in the Pre-Jurassic time to a thin (< 80-120 km) and hot (> 100 mW/m^2) lithosphere in the Cenozoic (Griffin *et al.*, 1998; Xu *et al*., 1998). Large-scale Jurassic-Cretaceous crustal extension in the Dabie-Tongbai Shan region was recognized by Hacker & Wang (1995), You *et al.* (1998) and Suo *et al.* (2000). We consider that the ~ 132 Ma migmatization, amphibolite-facies metamorphism and extensive magmatism in the NDU are all related to this significant Mid-Cretaceous lithospheric thermal event in eastern China, which was also responsible for the change of Pacific subduction from highly oblique to orthogonal (Yin & Nie, 1996; Ratschbacher *et al.*, 2000).

7. Conclusions

Zircon U-Pb results suggest that the migmatization in the NDU happened at *ca.*132 Ma before present, as a result of the important thermal event in eastern China yielded voluminous Yanshanian granitoids. The NDU was uplifted after the migmatization at a cooling rate of 10-12°C/Ma. The decoupling between the Rb-Sr age for biotite and $^{40}Ar/^{39}Ar$ age for hornblende may be attributed to the hornblende recrystallization induced by fluids after the migmatization. This study supports the existence of pre-Cretaceous or even Precambrian rocks in the NDU. Granulite-facies rocks tectonically overlie the NDU and represent scraps from the CDU and / or SDU. These rocks were metamorphosed at least 195 Ma ago, slightly later than or nearly coeval with the HP-UHP metamorphism, and therefore evidently predates the migmatization in the NDU. The different thermal histories between the granulites and migmatites suggest that the NDU and SDU/CDU may have different evolutionary histories.

Acknowledgments: Technical assistance for mineral separation, chemical analyzing and isotopic dating by Zheng Zhou, Zhixin Qian, Tongmo Dai, Ying Liu and Xianglin Tu at GIG-CAS, and Marty Grove at UCLA is gratefully appreciated. Constructive comments by Prof. An Yin at UCLA on an early version of this manuscript are gratefully appreciated. J.H.W. thanks the Chinese Academy of Sciences (CAS) and Prof. An Yin for supporting his visit to UCLA and using the argon lab. This work was co-supported by the National Natural Science Foundation of China (49472134 and 49333030), the National Climbing Plan Project (95-Y-25), Hong Kong RGC Grant (HKU7110/97P), and CAS's Special President Grant. We are grateful for insightful reviews by Prof. Rainer Altherr, Prof. Klaus Mezger and Dr. Anthi Liati, who helped us to clarify the manuscript.

References

Ames, L., Zhou, G., Xiong, B. (1996): Geochronology and isotopic character of ultrahigh-pressure metamorphism with implications for collision of the Sino-Korean and Yangtze cratons, central China. *Tectonics*, **15**, 472-489.

Baker, F. (1979): Trondhjemite: Definition, environment and hypotheses of origin. *In* "Trondhjemites, dacites and related rocks", F. Baker, ed. Elsevier, Amsterdam, 1-12.

Chavagnac, V. & Jahn, B. M. (1996): Coesite-bearing eclogite from the Bixiling complex, Dabie Mountains, China: Sm-Nd ages, geochemical characteristics and tectonic implication. *Chemical Geol.*, **133**, 29-51.

Chen, D.G., Isachsen, C., Zhi, X.C., Zhou, T.X., Cheng, H., Xia, Q.K. (2000): U/Pb ages for gneisses from Qianshan, Anhui. *Chinese Sci. Bull.*, **45**, 764-767.

Chen, D.G., Wang, X., Deloule, E., Li, B.X., Xia, Q.K., Cheng, H., Wu, Y.B (2001): The genesis of pyroxenites in the Northern Dabie Shan: U-Pb SIMS ages and compositions of zircons. *Chinese Sci. Bull.*, **46**, 586-590.

Chen, J.F., Xie, Z., Liu, S.S., Li, X.M., Foland, K.A. (1995): $^{40}Ar/^{39}Ar$ and fission-track dating the cooling age of the Dabie orogenic belt. *Sci. China (B)*, **25**, 1086-1092.

Chen, N.S., Sun, M., You, Z.D., Malpas, J. (1998): Well-preserved garnet growth zoning in granulite from the Dabie Mountains, central China. *J. metamorphic Geol.*, **16**, 213-222.

Chen, T.Y., Niu, B.G., Liu, Z.G. (1991): Isotopic geochronology of metamorphism and Yanshanian magmatism within the Dabie Shan. *Acta Geol. Sinica*, **65**, 329-335.

Chen, W.J., Harrison, T.M., Heizler, M.T., Liu, R., Ma, B., Li, J. (1992): The cooling history of melange zone in the north Jiangsu-south Shandong region: evidence from multiple diffusion-domain $^{40}Ar/^{39}Ar$ thermal geochronology. *Acta Petrol. Sinica*, **8**, 1-17.

Dai, T. & Hong, A. (1982): $^{40}Ar/^{39}Ar$ dating and some isotopic determinations on Himalaya biotites from granitoids rocks in southern Tibet. *Geochimica*, **11**, 48-55.

Defant, M.J. & Drummond, M.S. (1990): Derivation of some modern arc magmas by melting of the subducted lithosphere. *Nature*, **347**, 662-665.

DePaolo, D.J. (1988): Neodymium isotope geochemistry: An introduction. Springer-Verlag, Berlin, 181 p.

Eide, E.A., McWilliams, M.O., Liou, J.G. (1994): $^{40}Ar/^{39}Ar$ geochronology and exhumation of HP to UHP metamorphic rocks in east-central China. *Geology*, **22**, 601-604.

Faure, M., Lin, W., Shu, L.S., Sun, Y., Schärer, U. (1999): Tectonics of the Dabieshan (eastern China) and possible exhumation mechanism of ultra high-pressure rocks. *Terra Nova*, **11**, 251-258.

Ge, N.J., Hou, Z.H., Li, H.M., Chen, J.F, Liu, B., Ruan, J., Qin, L.P. (1999): Zircon U-Pb ages for the mafic-ultramafic pluton at Shacun (Yuexi) in the Dabie orogenic belt. *Chinese Sci. Bull.*, **44**, 2110-2114.

Geyh, M.A. & Schleicher, H. (1990): Absolute age determination: Physical and chemical dating methods and their application. Springer-Verlag, Berlin, 503 p.

Griffin, W.L., Zhang, A., O'Reilly, S.Y., Ryan, C.G. (1998): Phanerozoic evolution of the lithosphere beneath the Sino-Korean Craton. *In* "Mantle dymamics and plate interactions in east Asia", M.F.J. Flower, S.L. Chung, C.H. Lo, T.Y. Lee, eds. AGU, Washington D.C., 107-126.

Hacker, B.R. & Wang, Q.C. (1995): Thermal history of ultrahigh-pressure rocks, Dabie Mountains, China. *Tectonics*, **14**, 994-1006.

Hacker, B.R., Ratschbacher, L., Webb, L., Ireland, T., Walker, D., Dong, S.W. (1998): U/Pb zircon ages constrain the architecture of the ultrahigh-pressure Qinling-Dabie orogen, China. *Earth Planet. Sci. Lett.*, **161**, 215-230.

Harrison, T.M., Leloup, P.H., Ryerson, F.J., Tapponnier, P., Lacassin, R., Chen, W. (1996): Diachronous initiation of transtension along the Ailao Shan-Red River shear zone, Yunnan and Vietnam. *In* "The Tectonic Evolution of Asia", A. Yin & T.M. Harrison, eds. Cambridge University Press, Cambridge, 208-226.

Jahn, B.M., Wu, F.Y., Lo, C.H., Tsai, C.H. (1999): Crust-mantle interaction induced by deep subduction of the continental crust: geochemical and Sr-Nd isotopic evidence from post-collisional mafic-ultramafic intrusions of the northern Dabie complex, central China. *Chemical Geol.*, **157**, 119-146.

Jian, P., Zhang, Z.C., Zhu, J.P., Lu, H., Yang, W.R., Han, Y.J., Wang, L.S. (1997): The Dabie basement is older than 2800 Ma: Evidence from the zircon age of granulite from Huangtuling. *Acta Geosci. Sinica*, **18**, 65-67.

Krogh, T.E. (1973): A low-contamination method for hydrothermal decomposition of zircon and extraction of U and Pb for isotopic age determinations. *Geochim. Cosmochim. Acta*, **48**, 505-511.

__ (1978): Vapour transfer for the dissolution of zircons in a multi-sample capsule at high-pressure. *in* "Short papers of the 4th International Conference on Geochronology, Cosmochronology, and Isotope Geology, R.E. Zartman, ed. USGS Open-File Rep., **78-701**, 233-234.

Li, S.G., Hart, S.R., Zheng, S.G., Liu, D.L., Zhang, G.W., Guo, A.L. (1989): Timing of collision between the north and south China blocks - the Sm-Nd isotopic age evidence. *Sci. China (B)*, **32**, 1393-1400.

Li, S.G., Xiao, Y., Liu, D., Chen, Y., Ge, N., Zhang, Z., Sun, S.-S., Cong, B., Zhang, R.Y., Hart, S.R., Wang, S. (1993): Collision of the North China and Yangtze blocks and formation of coesite-bearing eclogites: timing and processes. *Chemical Geol.*, **109**, 89-111.

Li, S.G., Hong, J., Li, H.M., Jiang, L.L. (1999): U-Pb zircon ages of the pyroxenite-gabbro intrusions in Dabie Mountains and their geological implications. *Geol. J. China Univ.*, **5**, 351-355.

Li, S. & Wang, T. (1991): Geochemistry of granitoids in the Tongbai-Dabie Shan, central China. China University of Geosciences Press, Wuhan, 208 p.

Liou, J.G., Zhang, R.Y., Wang, X., Eide, E.A., Ernst, W.G., Maruyama, S. (1996): Metamorphsim and tectonics of high-pressure and ultrahigh-pressure belts in the Dabie-Sulu region, China. *In* "The Tectonic Evolution of Asia", A. Yin & T.M. Harrison, eds. Cambridge University Press, Cambridge, 301-344.

Ludwig, R.K. (1992): Isoplot-a plotting and regression program for radiogenic-isotope data, version 2.57. *U. S. Geol. Surv.*, *Open-File Rep.*, **91-445**, 40.

Maruyama, S., Liou, J.G., Zhang, R.Y. (1994): Tectonic evolution of the ultrahigh-pressure and high-pressure metamorphic belts from central China. *Island Arc*, **3**, 112-121.

Martin, H. (1999): Adakitic magmas: modern analogues of Archean granitoids. *Lithos*, **46**, 411-429.

McDougall, I. & Harrison, T.M. (1999): Geochronology and thermochronology by the $^{40}Ar/^{39}Ar$ method, Oxford University Press, New York, 1999, 269 p.

Mehnert, K.R. (1968): Migmatites and the origin of granitic rocks. Elsevier, Amsterdam, 388 p.

Okay, A.I., Xu, S., Senger, A.M.C. (1989): Coesite from the Dabie Shan eclogites, central China. *Eur. J. Mineral.*, **1**, 595-598.

Ratschbacher, L., Hacker, B.R., Webb, L.E., McWilliams, M., Ireland, T., Dong, S.W., Calvert, A., Chateigner, D., Wenk, H.-R. (2000): Exhumation of the ultrahigh-pressure continental crust in east central China: Cretaceous and Cenozoic unroofing and the Tan-Lu fault. *J. Geophys. Res.*, **105(B6)**, 13,030-13,338.

Rowley, D.B., Xue, F., Tucker, R.D., Peng, Z.X., Baker, J., Davis, A. (1997): Ages of ultrahigh pressure metamorphism and protolith orthogneisses from the eastern Dabie Shan: U/Pb zircon geochronolgy. *Earth Planet. Sci. Lett.*, **151**, 191-203.

Stacey, J.S. & Kramers, J.D. (1975): Approximation of terrestrial lead isotope evolution by a two-stage model. *Earth Planet. Sci. Lett.*, **26**, 207-221.

Steiger, R.H. & Jäger, E. (1977): Subcommission on Geochronology: Conventions on the use of decay constants in geo- and cosmochronology. *Earth Planet. Sci. Lett.*, **36**, 359-362.

Suo, S.T., Sang, L.K., Han, Y.J., You, Z.D., Zhong, Z.Q., Wang, J.H., Zhou, H.W., Zhang, Z.M. (1993): The petrology and tectonics in the Dabie Precambrain metamorphic terrain, central China. China University of Geosciences Press, Wuhan, 259 p.

Suo, S.T., Zhong, Z.Q. & You, Z.D. (2000): Post-UHP-metamorphic extension and the uplift process of UHP metamorphic rocks in the Dabie Block. *Sci. China (D)*, **30**, 9-17.

Wang, J.H. (1991): The early evolution of the Dabie Complex, with special reference to the genetic mechanism of migmatites. China University of Geosciences Press, Wuhan, 134 p.

Wang, J.H., Liu, W., Zhang, Y.X. (1992): Polyphase folding of supracrustal sequences in the Dabie complex in northeastern Hubei. *Regional Geol. China*, **11**: 141-145.

Wang, J.H., Sun, M., Chang, X.Y., Deng, S.X. (1997): Dynamic models for origin of the migmatites with thermal centers in the Dabie complex, Hubei, central China. *in* "Precambrain Geology and Metamorphic Petrology", X.L. Qian, Z.D. You, B.M. Jahn, H.C. Halls, eds., Procs. 30th IGC, 17, VSP, Zeist, 203-215.

Wang, J.H., Yin, A., Harrison, T.M., Grove, M., Zhang, Y.Q., Xie, G.H. (2001): A tectonic model for Cenozoic igneous activities in the eastern Indo-Asian collision zone. *Earth Planet. Sci. Lett.*, **188**, 123-133.

Wang, Q., Wang, R.J. Qiu, J.X., Zhao, Z.H., Sang, L.K., Hu, Z.X., Dai, S.Q., He, Y., Zhou, G.H., Xu, W., Wang, J.X., Qi, X.M., Zhang, S.J. (2000a): Petrogenesis of Jiuzihe granites in the core of Dabie Mountains. *Geochimica*, **29**, 120-131.

Wang, Q., Xu, J.F., Wang, J.X., Zhao, Z.H., Wang, R.J., Qiu, J.X., Xiong, X.L., Sang, L.K., Peng, L.H. (2000b): The recognification of adakite-type gneisses in the North Dabie Mountain and its implication to the UHP metamorphic geology. *Chinese Sci. Bull.*, **45**, 1927-1933.

Wang, X., Liou, J.G., Mao, H.K. (1989): Coesite-bearing eclogites from the Dabie Mountains in central China. *Geology*, **17**, 1085-1088.

Xu, S., Okay, A.I., Ji, S., Sengor, A.M.C., Su, W., Jiang, L. (1992): Diamond from the Dabie Shan metamorphic rocks and its implication for the tectonic setting. *Science*, **256**, 80-82.

Xu, X., O'Reilly, S.Y., Griffin, W.L., Zhou, X., Huang, X. (1998): The nature of the Cenozoic lithosphere at Nushan, eastern China. *In* "Mantle dymamics and plate interactions in east Asia", M.F.J. Flower, S.L. Chung, C.H. Lo, T.Y. Lee, eds. Geodynamics Series, **27**, AGU, Washington D.C., 167-195.

Xue, F., Rowley, D.B., Yucker, R.D., Peng, Z.X. (1997): U-Pb zircon ages of granitoids rocks in the North Dabie Complex, eastern Dabie Shan, China. *J. Geol.*, **105**, 744-753.

Yin, A. & Nie, S. (1996): A Phanerozoic palinspastic reconstruction of China and its neighboring regions. *In* "The Tectonic Evolution of Asia", A. Yin & T.M. Harrision, eds. Cambridge University Press, New York, 442-485.

You, Z.D., Suo, S.T., Zhong, Z.Q., Zhang, Z.M., Wei, B.Z. (1998): The extensional tectonics and retrometamorphic processes subsequent to the HP-UHP metamorphic events in Dabieshan, China. *Continental Dynamics*, **3**, 63-71.

Zhang, J.F., Jin, Z.M., Green II, H.W., Jin, S.Y. (2000): Water in the deep subduction zone: an evidence from the UHP eclogites from the Dabie Shan. *Chinese Sci. Bull.*, **45**, 1889-1894.

Zhang, R.Y., Liou, J.G., Tsai, C.H. (1996): Petrogenesis of a high-temperature metamorphic terrain: a new interpretation for the north Dabie Shan, central China. *J. metamorphic Geol.*, **14**, 319-333.

Zheng, X.S., Jin, C.W., Zhai, M.G. (2000): Approach to the source of the gray gneisses in North Dabie terrain: Sm-Nd isochron age and isotope compositions. *Acta Petrol. Sinica*, **16**, 194-198.

Zheng, X.S., Jin, C.W., Zhai, M.G., Shi, Y. (1999): Petrochemistry and tectonic background of the gray gneisses in North Dabie terrane. *Acta Petrol. Sinica*, **15**, 350-358.

Zhou, C.T., Tang, J.F., Gao, T.S., Lu, R.K. (1995): The formation and geochronology of the basement gneisses of the Dabie Mountains. *Geol. Anhui*, **5**, 29-40.

Zhu, B.Q., Li, X.H., Dai, D.M., Chen, Y.W., Fan, S.K., Gui, X.T., Wang, H.F. (1998): The theory of isotope systems in earth sciences and its application. Science Press, Beijing, 330 p.

Received 20 November 2000
Modified version received 20 June 2001
Accepted 29 November 2001